

ARTICLES

Theoretical Study of the Oxidation Reactions of Methacrylic Acid and Methyl Methacrylate by Triplet O₂Guixiu Wang,[†] Dongju Zhang,^{*,†} Xiaohong Xu,[†] and Jianhua Zhou[‡]*Institute of Theoretical Chemistry, Shandong University, Jinan 250100, P. R. China, and Department of Chemical Engineering, Shandong Institute of Light Industry, 250353, P. R. China**Received: July 13, 2006; In Final Form: November 30, 2006*

The oxidations of organic compounds and polymers by triplet O₂ were called “dark oxidation” or “auto-oxidation”, in contrast to their “photo-oxidation” by singlet O₂. To study the relevant dark oxidation mechanism we take methacrylic acid (MAA) and methyl methacrylate (MMA) as prototypes to study their reactions with triplet O₂ by performing density functional theory calculations. Two reaction channels, the C–H bond oxidation and C=C bond oxidation, have been characterized in detail. The structures of the initial contact charge-transfer complexes, intermediates, transition states, and final oxides involved in the reactions have been localized at the UB3LYP/6-311+G(d,p) level. It is found that the C–H bond in the methyl group connected to the C=C bond presents relatively higher reactivity toward triplet O₂ than the C=C bond itself. Thus, the reactions are expected to proceed via the C–H bond oxidation branch at room temperature and also via C=C bond oxidation at elevated temperature. In this sense, an effective method for preventing or retarding the dark oxidations of MAA and MMA in a natural environment is to chemically decorate or protect the C–H bond in the methyl connected to the C=C bond. The present results are expected to provide a general guide for understanding the dark oxidation mechanism of organic compounds and polymers.

1. Introduction

Oxidation reactions of organic compounds and polymers in a natural environment have been observed for 100 years.¹ These reactions were called “dark or auto-oxidation reactions” of organic compounds and polymers since they involve ground-state (triplet) O₂ and occur under conditions without light and any additional excitement, in contrast to the corresponding photocatalytic oxidation reactions involving excited-state (singlet) O₂.² Thus far the mechanism of the dark oxidation reactions has remained less known, although a lot of experimental research in this area has been carried out.^{3–6}

Methacrylic acid (MAA) and methyl methacrylate (MMA) are important unsaturated organic compounds. They and their polymers play substantial roles in chemical industry. MAA can be used to make dope, insulating materials, bond, and ion-exchange resin. MMA is also called organic glass since it is often used as a substitute for glass due to its unique properties, such as high transparency, cheap prices, and easy processing. Both MAA and MMA, however, can be slowly oxygenated under ambient conditions to form the corresponding peroxides. As early as 1958 Frank and Miller⁷ observed the oxidation of MMA by triplet O₂ while studying the effect of oxygen on polymerization of MMA. They found that the presence of oxygen strongly retarded the polymerization reaction since it oxidized MMA into peroxides, methyl pyruvate, and formaldehyde. However,

the relevant oxidation mechanism was not given. Subsequently, Feng et al. studied the dark oxidation reactions of a series of organic compounds,^{8–13} including MAA and MMA,⁸ ethers,¹³ cumene, and polystyrene⁹ to understand the dark oxidation mechanisms. By determining the electronic absorbing spectra of these model compound systems, they observed the existence of the initial contact charge-transfer complexes (CCTCs) as well as the final hydroperoxides (HPs). These experimental studies have provided useful information for understanding the dark oxidation reactions of organic compounds and polymers; however, the details of the mechanism and structures of CCTCs are still not very clear. To model the dark oxidation reactions of organic compounds and polymers, here we take the reactions of MAA and MMA with triplet O₂ as prototypes to study the detailed reaction mechanism by performing quantum chemistry calculations. For the chosen prototype systems we are interested in the following questions. (1) What are the structures and properties of the initial CCTCs and final HPs observed early? (2) Which bonds or groups in MAA and MMA are oxidized easily by triplet O₂, and what is the effective way to retard or stop them being oxidized? (3) What are the formation mechanisms of peroxides, methyl pyruvate, and formaldehyde, which were observed in experiments,^{7–13} from the reactions of MAA and MMA with triplet O₂? And (4) how are the detailed profiles of the potential-energy surfaces (PESs) for the reactions of MAA and MMA with triplet O₂? In the following we describe our theoretical procedures and discuss the calculated results. We expect that the present results may provide a general profile of

* To whom correspondence should be addressed. E-mail: zhangdj@sdu.edu.cn.

[†] Shandong University.

[‡] Shandong Institute of Light Industry.

the dark oxidation reactions of unsaturated organic compounds and their corresponding polymers.

2. Computational Method

Density functional theory (DFT) is reaching widespread use in calculations of quite sizable organic and inorganic molecules. In particular, B3LYP^{14–16} calculations have been shown numerous times in the literature to be successful for modeling systems containing C, H, and O atoms.^{17–20} In the present work, we checked the performances of two functionals, B3LYP and PW91, for describing the reactions of MAA and MMA with triplet O₂. The calculated results show that the PW91 functional is not able to provide appropriate geometrical structures for some of intermediates involved in the concerned reactions. For this reason, we chose the B3LYP functional with the standard 6-311+G(d,p) basis set, which is flexible enough to give a good account of longer range intermolecular interactions. Combination of the B3LYP functional and 6-311+G(d,p) can offer a good compromise between speed and accuracy for obtaining reliable thermodynamic and kinetic data of many reactions.²⁰

The structures of various species involved in the reactions of MAA and MMA with triplet O₂, including the reactants, transition states, intermediates, and products, were fully optimized without any symmetrical restriction. Harmonic vibrational frequencies were calculated at the same level for all stationary points to identify the nature (minima or first-order saddle points) of these species and provide zero-point vibrational energy (ZPE) corrections. The atomic charge assignments were based on natural bond orbital (NBO) analysis. The intrinsic reaction coordinate (IRC)²¹ paths were traced in order to verify the pathways between the transition states and the corresponding minima. The basis set superposition errors (BSSE) have been corrected by standard counterpoise method. To obtain the accurate relative energy, a single-point calculation for each structure optimized at the B3LYP/6-311+G(d,p) level was again calculated at the MP2/6-311+G(d,p) level. Because singlet O₂ is higher in energy than triplet O₂ by only 0.98 eV (22.60 kcal/mol),²² the singlet–triplet interstate crossing for the reactions considered here may occur on the PESs. We addressed this issue in the present work by performing calculations for the relevant singlet species and searching for possible crossing points between the two PESs of different spin states. All calculations were implemented using the Gaussian 03 package.²³

We checked the accuracy of the chosen UMP2/6-311+G(d,p)//UB3LYP/6-311+G(d,p) level by calculating the ground-state properties of triplet O₂. The calculated the bond length, binding energy, and vibration frequency at this level are 1.206 Å, 5.15 eV, and 1633 cm⁻¹, respectively. The results compare well the experimental values^{24,25} of 1.21 Å, ~5.12 eV, and 1580 cm⁻¹. In addition, we find that at the chosen level of theory the deviations of *S*² expectation values for the open-shell species involved here are small and never exceed 5%, indicating that spin contaminations resulting from the present calculations are negligible.

3. Results and Discussion

Optimized structures for various possible species involved in the reactions of MAA and MMA with triplet O₂ are shown in Figures 1–3, the profiles of PESs are shown in Figure 4, and the relevant energies are listed in Table 1. For all cited relative energies, ZPE and BSSE corrections have been taken into account.

3.1. Contact Charge-Transfer Complexes. The contact charge-transfer complexes (CCTCs) we are talking about mean

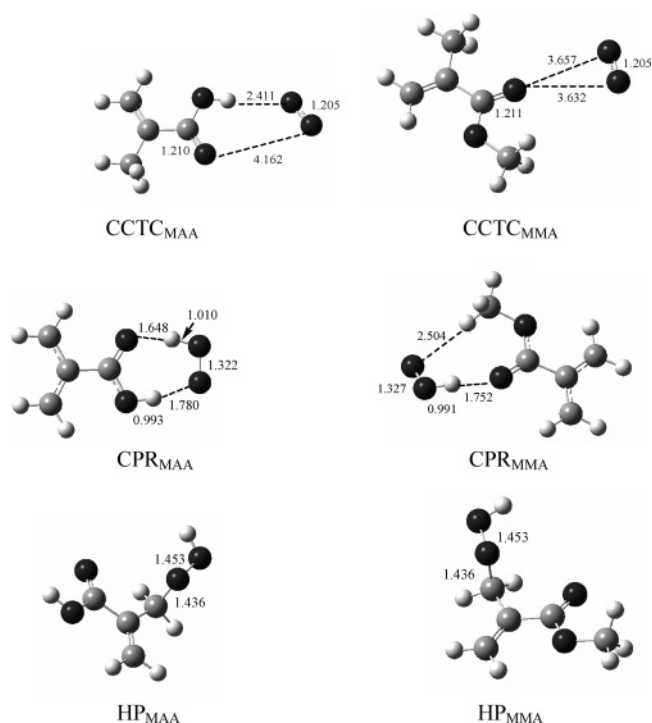


Figure 1. Structures of the most stable contact charge-transfer complexes (CCTCs), cage-like pairs of radicals (CPRs), and hydroperoxides (HPs) involved in the C–H bond oxidation branches for the reactions of MAA (MMA) with triplet O₂, optimized at the UB3LYP/6-311+G(d,p) level. The gray, black, and white balls denote C, O, and H atoms, respectively.

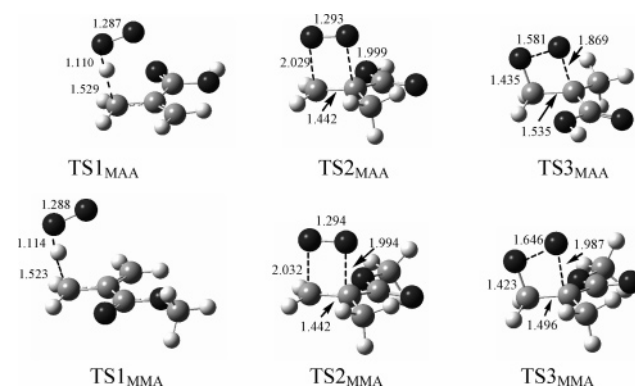


Figure 2. Transition-state structures involved in the two possible pathways (C=C bond oxidation and C–H bond oxidation) for the reactions of MAA (MMA) with triplet O₂, optimized at the UB3LYP/6-311+G(d,p) level. The gray, black, and white balls denote C, O, and H atoms, respectively.

the simple complexes formed between organic compounds and triplet O₂ in the initial stages of the reactions. This notion has been used in academics since it was first discussed by Evans³ in 1953 when he observed that triplet O₂ could form a loosely connected complex with organic compounds. To ascertain the structural details of the CCTCs of MAA and MMA with triplet O₂, we considered their various possible geometrical structures by setting an O₂ molecule at different positions of MAA and MMA, such as near the C=C bond, ether group, methyl group, methylene group, and carbonyl. Upon optimization, the relaxed structures generally resemble the initial inputs. By comparing the total energies of geometrically different CCTCs, we identified the energetically favorable CCTC structures for MAA and MMA with triplet O₂, denoted as CCTC_{MAA} and CCTC_{MMA}, as shown in Figure 1. These most stable CCTCs are considered as appropriate structures for the following oxidation reactions.

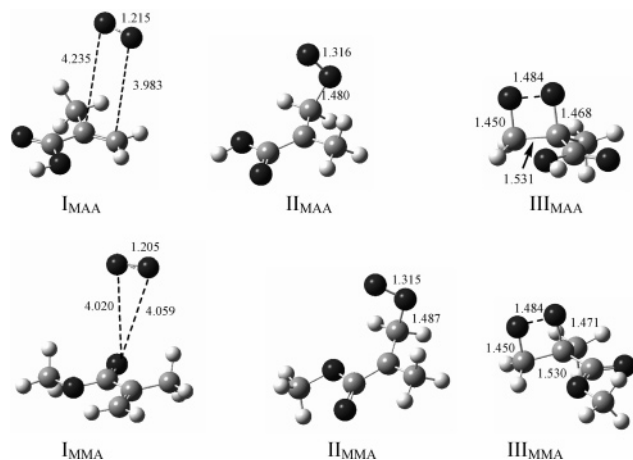


Figure 3. Possible intermediates and products involved in the reactions of MAA (MMA) with triplet O_2 , optimized at the UB3LYP/6-311+G(d,p) level. The gray, black, and white balls denote C, O, and H atoms, respectively.

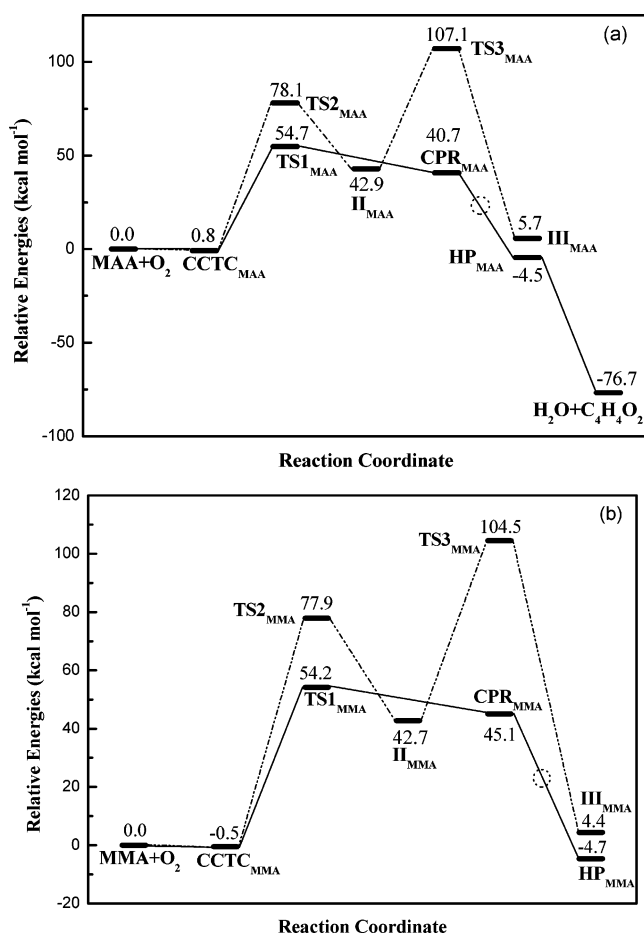


Figure 4. Profiles of the potential-energy surfaces along both the C–H bond oxidation branch (connected by solid lines) and C=C bond oxidation branch (connected by dotted lines) for (a) reaction of MAA with triplet O_2 and (b) reaction of MMA with triplet O_2 , calculated at the UMP2/6-311+G(d,p)/UB3LYP/6-311+G(d,p) level.

From the structural parameters shown in Figure 1 we find that the distances between MAA (MMA) and O_2 are large. Both the MAA (MMA) and O_2 units in CCTC_{MAA} and CCTC_{MMA} almost remain the geometrical structures of isolated molecules. For example, the lengths of the C=O and O=O in CCTC_{MAA} are 1.210 and 1.205 Å, which are almost the same with those in isolated MAA and O_2 . On the other hand, our calculations indicate that the binding energies of CCTC_{MAA} and CCTC_{MMA}

with respect to the isolated reactants are only 0.8 and 0.5 kcal mol⁻¹, respectively. NBO population analyses show that the electronic charge transfers from the lone pair electrons on the carbonyl O atom in MAA (MMA) to the π^* orbital in O_2 are also very small. In this sense, the initial complexes should be described as simple van der Waals complexes rather than so-called “CCTCs”. However, we still use the idiom of CCTCs to name these initial complexes, although it is not very appropriate to describe their nature. The weak interactions between MAA (MMA) and O_2 are in good agreement with the experimental findings^{8–13} that the formation of CCTCs is slow and reversible at room temperature.

3.2. Reaction Mechanisms. To understand the oxidation mechanism of MAA and MMA by triplet O_2 we considered several possible reaction pathways and performed detailed potential-energy surface (PES) scans to locate the minima and first-order saddle points on the PESs. The calculated results show that the dark oxidation reactions may proceed via two possible pathways which involve C–H and C=C bond oxidation of MAA and MMA, respectively, as shown in Scheme 1. The optimized transition-state structures involved in the two pathways are depicted in Figure 2, where TS1 involves C–H bond oxidation via H-atom abstraction and TS2 and TS3 correlate with C=C bond oxidation. Formation of CCTCs was found to be a viable initial step for both C–H and C=C bond oxidation. In the following discussion we focus our attention on one of the two reactions concerned, reaction of MAA with triplet O_2 , while for reaction of MMA with O_2 we only show the optimized structures in Figures 1–4 and list corresponding energies in Table 1 for simplification, and the relevant details are less involved in view of its large similarity to the former.

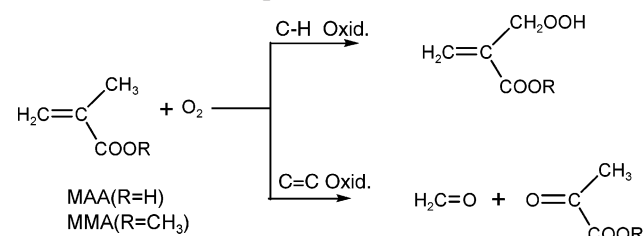
3.2.1. C–H Bond Oxidation via an H-Abstraction Mechanism. The H atom in the methyl group connected to the C=C bond of MAA is expected to have higher reactivity toward ground-state O_2 than other H atoms due to the effective conjugative effect between the σ electrons in the C–H bond and the π electrons of the C=C bond, which results in the σ electrons in the C–H bond being highly delocalized and hence the reactivity of the H atom is enhanced. The present calculations have confirmed this conjecture. We optimized various transition-state structures for the reactions of different C–H bonds in MAA with triplet O_2 and found that the C–H bond in the methyl group connected to the C=C bond is oxidized most easily via an H-abstraction mechanism. From the structural parameters shown in Figure 2 it is clear that TS1_{MAA} is a late saddle point on the PES, where the forming O–H bond is 1.110 Å and the breaking C–H bonds are 1.529 Å. The relative energy is 54.7 kcal mol⁻¹ above the isolated reactants, and the imaginary vibrational frequency is 1253i. The transition vectors associated with the imaginary frequency and the geometry of the transition structure are completely consistent with the notion of H-atom abstraction. By performing IRC calculations we confirmed that the forward product from TS1_{MAA} is CCTC_{MAA} while the reverse product is a cage-like pair of radicals CPR_{MAA}, as shown in Figure 1. CPR_{MAA} is less stable by 40.7 kcal mol⁻¹ than the corresponding isolated reactants, indicating these cage-like pairs of radicals are instantaneously stable structures formed between the dehydrogenated organic radicals and newly forming OOH radical via hydrogen bonds. It is noted that a planar seven-membered ring structure is formed in CPR_{MAA} via two hydrogen bonds with distances of 1.648 and 1.780 Å, respectively (Figure 1). The structural parameters of the OOH radical unit in CPR_{MAA} are obviously different from those in CPR_{MMA} due to the existence of the double hydrogen-bond structure. In CPR_{MAA}

TABLE 1: Total Energies (E , in hartrees) and Relative Energies (ΔE , in kcal mol⁻¹) for Various Species Involved in Reactions of MMA (MAA) with Triplet O₂, Calculated at the UMP2/6-311+G(d,p)//UB3LYP/6-311+G(d,p) Level

	species ^a	E^b (au)	ΔE^c (kcal mol ⁻¹)	ZPE (kcal mol ⁻¹)	BSSE (kcal mol ⁻¹)	
MAA + O ₂	MAA + O ₂	-455.7789766	0.0	61.9	0.0	
	CCTC _{MAA}	-455.7811887	-0.8	62.2	0.3	
	TS1 _{MAA}	-455.6881547	54.7	58.7	0.9	
	CPR _{MAA}	-455.7152039	40.7	61.9	0.7	
	HP _{MAA}	-455.7931235	-4.5	64.8	1.5	
	H ₂ O + C ₄ H ₄ O ₂ ^d	-455.9058255	-76.7	63.8	1.0	
	TS2 _{MAA}	-455.6570201	78.1	62.0	1.5	
	I _{MAA}	-455.7152119	42.9	63.3	1.5	
	TS3 _{MAA}	-455.6153289	107.1	62.5	3.8	
	III _{MAA}	-455.7779412	5.7	65.4	1.6	
	MMA+O ₂	MMA+O ₂	-494.9563171	0.0	79.3	0.0
		CCTC _{MMA}	-494.9577752	-0.5	79.5	0.2
		TS1 _{MMA}	-494.8662806	54.2	76.1	0.9
CPR _{MMA}		-494.8849290	45.1	78.9	0.7	
HP _{MMA}		-494.9707621	-4.7	82.2	1.5	
TS2 _{MMA}		-494.8346616	77.9	79.4	1.5	
I _{MMA}		-494.8928804	42.7	80.7	1.5	
TS3 _{MMA}		-494.7938318	104.5	80.0	1.8	
III _{MMA}		-494.9559008	4.4	82.8	1.6	

^a Involved in the dark oxidation reactions. ^b ZPEs have been included. ^c ZPE and BSSE corrections have been taken into account. ^d C₂H₄O₂ denotes 2-carboxy acrolein generated from HP_{MAA}.

SCHEME 1: Possible Pathways for the Reactions of MAA (MMA) with Triplet O₂



the O–O and O–H bond lengths are 1.322 and 1.010 Å, respectively. Once the metastable radical is formed, it would couple quickly to form the energetically favorable HP_{MAA}, which is shown in Figure 1. It should be noted that the ground state of HP_{MAA} is in the singlet state, and thus, its formation demands an intersystem crossing between the triplet and singlet surfaces, as indicated by the dotted cycle in Figure 4. The interstate crossing between the singlet and triplet will be discussed in the last section of this work. HP_{MAA} is calculated to be 4.5 kcal mol⁻¹ more stable than the isolated reactants. Clearly, the total dark oxidation reaction of MAA with O₂ is exothermic, although they initially need to overcome a high barrier of 54.7 kcal mol⁻¹. Once the reaction is initiated, however, the accumulative heat would make the reaction proceed continually and slowly. It is noted that HP_{MAA} was not observed in the experiment.⁸ It could be that it was quickly dissociated into 2-carboxy acrolein (C₄H₄O₂) and a water molecule under acidic conditions.⁸ Our calculated results indicate that the dissociation products are energetically more favorable by 76.7 kcal mol⁻¹ than HP_{MAA}. The PES profile for the dark oxidation reaction of MAA with triplet O₂ along the C–H bond oxidation pathway is shown in Figure 4a with the thin solid line.

3.2.2. C=C Bond Oxidation Mechanism. The transition-state structures of the reaction of MAA with triplet O₂ along the C=C bond oxidation branch, TS2_{MAA} and TS3_{MAA}, are collected in Figure 2, and the corresponding minima obtained by performing IRC calculations from them, denoted as I_{MAA}, II_{MAA}, and III_{MAA}, are shown in Figure 3. From the structural parameters shown in Figure 2 and the corresponding transition vectors associated with the imaginary frequencies, it is very clear that O₂ in TS2_{MAA} is attacking the C=C bond. The C–C and

O–O distances in TS2_{MAA} are elongated to 1.442 and 1.293 Å compared to those in the corresponding free molecules (1.337 and 1.206 Å), and the C–O distances are 1.999 and 2.029 Å, indicating the π bonds of C=C and O=O are being broken and the C–O bond is being formed. The imaginary vibrational frequency of TS2_{MAA} is 720i. IRC calculation allows us to find the minima connected by TS2_{MAA}: intermediates I_{MAA} and II_{MAA}, which correspond to the initial complexes between MAA and O₂ and the adduct oxides between MAA and O₂, respectively. The relative energy of TS2_{MAA} is 78.1 above the isolated reactants, and that of the corresponding adduct oxide II_{MAA} is 42.9 kcal mol⁻¹. This oxide can further be converted into intermediate III_{MAA} via TS3_{MAA} with a barrier of 64.2 kcal mol⁻¹. The imaginary vibrational frequency of TS3_{MAA} is 3016i. From the structural parameters shown in Figure 2 and the transition vector associated with the imaginary frequency for TS3_{MAA}, it is very clear that the second C–O σ bond is being formed with a C–O distance of 1.869 Å and the O–O and C–C σ bonds are being broken with distances of 1.581 and 1.535 Å, respectively. The forward minimum from TS3_{MAA} is intermediate III_{MAA}, which further dissociates into formaldehyde and pyruvate. However, it should be noted that these products will occur on the singlet surface via an intersystem crossing between triplet and singlet during dissociation.

3.2.3. Comparison of C–H and C=C Bond Oxidations. According to the results above, we summarized both the C–H and C=C bond oxidation branches into Figure 4a and b for the two systems considered here. Clearly, the PES profiles for reactions of MAA and MMA with triplet O₂ are very alike, though small differences exist in the relative energies of the corresponding species, as expected from the similar reaction mechanisms of MAA and MMA toward triplet O₂. Comparing the C–H bond oxidation branch with the C=C bond oxidation branch for each system we find that the former, which results in formation of HPs, is energetically more favorable than the latter, which dissociates MAA (MMA) into formaldehyde and pyruvate (pyruvate ester). However, the latter is expected to be a viable reaction channel at elevated temperature. The results support the early experimental finding by Frank and Miller⁷ that the products of oxidation from the reaction of MMA with oxygen at 50 °C consist of 80% HP and 20% methyl pyruvate and formaldehyde.

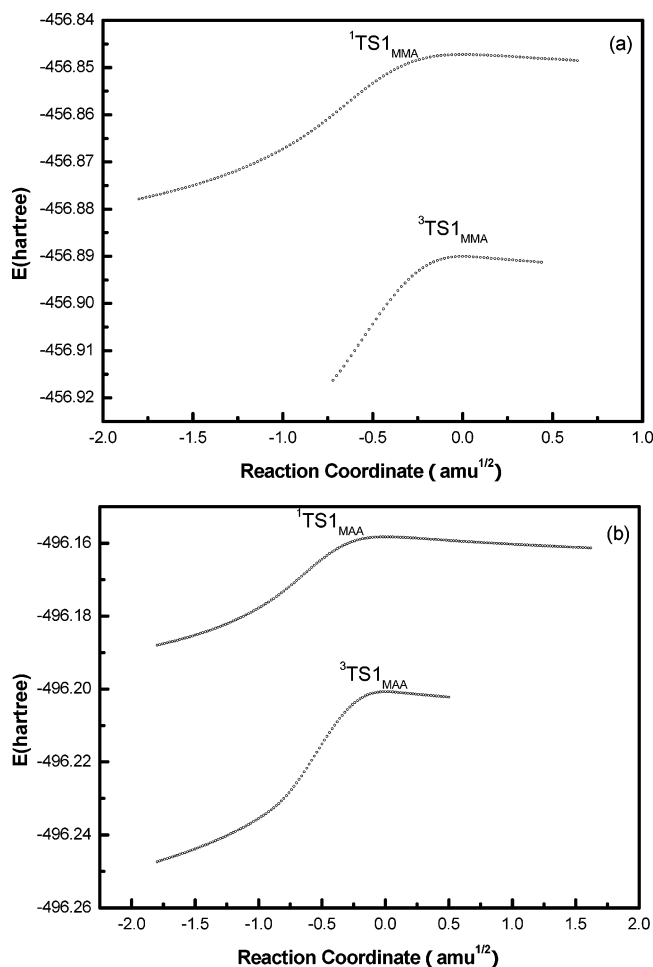


Figure 5. Potential-energy profiles of the triplet and singlet PESs along the reaction coordinates (a) in the vicinity of TS1_{MAA} and (b) in the vicinity of TS1_{MMA} . Superscripts 1 and 3 denote spin multiplicity.

From the present calculations the C=C bond oxidation pathway is not competitive with that of the C-H bond oxidation; thus, the latter is mainly responsible for the observed dark oxidations of MAA and MMA by oxygen at room temperature. Thus, an effective method for preventing or retarding the dark oxidation of MAA and MMA could be to chemically decorate or protect the C-H bond in the methyl connected to the C=C bond.

3.3. Singlet-Triplet Intersystem Crossing. In this section we discuss the possible crossing between the triplet-singlet PESs, which are a crucial issue for reactions involving triplet O_2 . It is known that spin inversion can generally occur in the vicinity of a crossing seam of two PESs of different spin multiplicities.²⁶⁻²⁷ As shown in Figure 4, the calculated reaction barriers for reactions of MAA (MMA) with triplet O_2 are ca. 54 kcal mol⁻¹, which is larger than the singlet-triplet energy splitting of O_2 (22.60 kcal mol⁻¹).²² In this sense it seems possible that the crossing seam between the triplet-singlet PESs occurs in the vicinity of the entrance channel. To see the possible crossing at this region, we performed calculations for the singlet TS1_{MAA} and TS1_{MMA} . However, the resulting data indicate that their energies are higher by 13.41 and 13.77 kcal mol⁻¹ than the corresponding triplet counterparts, although the geometrical structures on the singlet PESs are similar to those on the triplet PESs. Further, we checked the singlet and triplet PESs around the entrance channels in detail by performing IRC calculations. As shown in Figure 5, the singlet IRC valleys always lie above the triplet ones in the vicinity of TS1_{MAA} (TS1_{MMA}), and thus,

the reactions would preferentially proceed on the triplet surfaces and do not involve interstate crossing until the CPRs are formed. As mentioned above, the CPRs are metastable radical and would couple quickly to form the energetically favorable singlet HP_{MAA} via the triplet-singlet intersystem crossing. To illustrate the crossing seams in the vicinity of the exit channels, we tried to optimize the structures of CPRs and HPs on both the triplet and singlet PESs. Our attempts, however, at obtaining singlet CPRs and triplets HPs were always unsuccessful. The initial guessed singlet CPRs always converge to the HPs upon optimization, while the imaged triplet HPs are always taken to the CPRs after relaxation. Therefore, we believe that in the vicinity of the existing channels there exists a triplet-singlet intersystem crossing that bears heavily on the product makeup.

4. Conclusions

DFT calculations for the reactions of MAA and MMA with triplet O_2 have been performed in detail to study the relevant dark oxidation mechanisms. Calculated results show that the dark oxidation reactions proceed via a C-H bond oxidation mechanism at room temperature and also via a C=C bond oxidation mechanism at elevated temperature. The structures and properties of all stationary points involved on the PESs, including initial contact charge-transfer complexes, intermediates, transition states, and final oxides, have been shown in detail. Chemically decorating or protecting the C-H bond in the methyl connected to the C=C bond may be an effective way to prevent or retard the dark oxidation of MAA and MMA at room temperature. The present results are expected to provide a guide to understanding the mechanisms of dark oxidation of unsaturated organic materials and their corresponding polymers.

Acknowledgment. This research was supported by the National Science Foundation of China (No. 20473047) and the Natural Science Foundation of Shandong Province (Nos. Y2004F04 and Y2006B42). The allocations of supercomputing time at the High Performance Computational Center of Shandong University are gratefully acknowledged. We thank the referees for their constructive comments which were used to improve the quality and significance of our manuscript.

References and Notes

- (1) Schönbein, M. R. *J. Chem. Soc.* **1851**, 4, 134.
- (2) Ranby, B.; Rabek, J. F. *Photodegradation Photo-oxidation and Photostabilization of Polymers*, John Wiley & Sons, Inc.: New York, 1975.
- (3) Evans, D. F. *J. Chem. Soc.* **1953**, 345-347.
- (4) Kulevsky, N.; Wang, C. T.; Stenberg, V. I. *J. Org. Chem.* **1969**, 34, 1345-1348.
- (5) Maeda, K.; Nakane, A.; Tsubomura, H. *Bull. Chem. Soc. Jpn.* **1975**, 48, 2448-2450.
- (6) Sonntag, C. V.; Neuwald, K.; Schuchmann, H. P.; Weeke, F.; Janssen, E. *J. Chem. Soc., Perkin Trans. II* **1975**, 171-175.
- (7) Frank, R. M.; Miller, A. A. *J. Am. Chem. Soc.* **1958**, 80, 2493-2496.
- (8) Dong, Y. P.; Qiu, K. Y.; Feng, X. D. *Chem. J. Chin. Univ. (in Chinese)* **1996**, 12, 1944-1947.
- (9) Zhu, J. M.; Cao, W. Y.; Feng, X. D. *Acta Polym. Sin. (in Chinese)* **1998**, 2, 252-255.
- (10) Dong, Y. P.; Qiu, K. Y.; Feng, X. D. *Chem. J. Chin. Univ. (in Chinese)* **1996**, 17, 1792-1795.
- (11) Zhu, J. M.; Cao, W. Y.; Feng, X. D. *Acta Polym. Sin. (in Chinese)* **1998**, 5, 632-636.
- (12) Zhu, J. M.; Cao, W. Y.; Feng, X. D. *Chem. J. Chin. Univ. (in Chinese)* **1998**, 19, 1181-1183.
- (13) Zhu, J. M.; Cao, W. Y.; Feng, X. D. *Chin. Chem. Lett.* **1997**, 8, 869-871.
- (14) Becke, A. D. *J. Chem. Phys.* **1993**, 98, 5648-5652.
- (15) Lee, C.; Yang, W.; Parr, R. G. *Phys. Rev. B.* **1988**, 37, 785-789.
- (16) Hehre, W. J.; Radom, L.; Schleyer, P. v. R.; Pople, J. A. *Ab Initio Molecular Orbital Theory*; John Wiley and Sons: New York, 1986.

- (17) Pisano, L.; Farriol, M.; Asensio, X.; Gallardo, I.; Gonzalez-Lafont, A.; Lluch, J. M.; Marquet, J. *J. Am. Chem. Soc.* **2002**, *124*, 4708–4715.
- (18) Barterberger, M. D.; Olson, L. P.; Houk, K. N. *Chem. Res. Toxicol.* **1998**, *11*, 710–711.
- (19) Leach, A. G.; Houk, K. N. *J. Am. Chem. Soc.* **2002**, *124*, 14820–14821.
- (20) Pfaendtner, J.; Yu, X.; Broadbelt, L. J. *J. Phys. Chem. A* **2006**, *110*, 10863–10871.
- (21) Fukui, K. *J. Phys. Chem.* **1970**, *74*, 4161–4163.
- (22) Weissbluth, M. *Atoms and Molecules*; Academic Press: New York, 1978; p. 587.
- (23) Frisch, M. J.; Trucks, G. W.; Schlegel, H. B.; Scuseria, G. E.; Robb, M. A.; Cheeseman, J. R.; Zakrzewski, V. G.; Montgomery, J. A., Jr.; Stratmann, R. E.; Burant, J. C.; Dapprich, S.; Millam, J. M.; Daniels, A. D.; Kudin, K. N.; Strain, M. C.; Farkas, O.; Tomasi, J.; Barone, V.; Cossi, M.; Cammi, R.; Mennucci, B.; Pomelli, C.; Adamo, C.; Clifford, S.; Ochterski, J.; Petersson, G. A.; Ayala, P. Y.; Cui, Q.; Morokuma, K.; Malick, D. K.; Rabuck, A. D.; Raghavachari, K.; Foresman, J. B.; Cioslowski, J.; Ortiz, J. V.; Baboul, A. G.; Stefanov, B. B.; Liu, G.; Liashenko, A.; Piskorz, P.; Komaromi, I.; Gomperts, R.; Martin, R. L.; Fox, D. J.; Keith, T.; Al-Laham, M. A.; Peng, C. Y.; Nanayakkara, A.; Gonzalez, C.; Challacombe, M.; Gill, P. M. W.; Johnson, B.; Chen, W.; Wong, M. W.; Andres, J. L.; Gonzalez, C.; Head-Gordon, M.; Replogle, E. S.; Pople, J. A. *Gaussian 03*, Revision B.05; Gaussian, Inc.: Pittsburgh, PA, 2003.
- (24) Huber, K. P.; Herzberg, G. *Molecular Spectra and Molecular Structure*; Van Nostrand Reinhold: New York, 1979.
- (25) Levine, I. N. *Molecular Spectroscopy*; John Wiley and Sons, Inc.: New York, 1975.
- (26) Kato, S.; Jaffe, R. L.; Komornicki, A.; Morokuma, K. *J. Chem. Phys.* **1983**, *78*, 4567–4580.
- (27) Yarkony, D. R. *J. Chem. Phys.* **1990**, *92*, 2457–2457–2463.